Chronology of Fluctuating Sea Levels Since the Triassic

BILAL U. HAQ, JAN HARDENBOL, PETER R. VAIL*

Advances in sequence stratigraphy and the development of depositional models have helped explain the origin of genetically related sedimentary packages during sea level cycles. These concepts have provided the basis for the recognition of sea level events in subsurface data and in outcrops of marine sediments around the world. Knowledge of these events has led to a new generation of Mesozoic and Cenozoic global cycle charts that chronicle the history of sea level fluctuations during the past 250 million years in greater detail than was possible from seismic-stratigraphic data alone. An effort has been made to develop a realistic and accurate time scale and widely applicable chronostratigraphy and to integrate depositional sequences documented in public domain outcrop sections from various basins with this chronostratigraphic framework. A description of this approach and an account of the results, illustrated by sea level cycle charts of the Cenozoic, Cretaceous, Jurassic, and Triassic intervals, are presented.

FOR MORE THAN A CENTURY, EARTH scientists have accumulated geologic evidence indicating fluctuations in the mean sea level during Phanerozoic time. In the early 20th century, Suess (*1*) remarked on the apparently synchronous episodes of deposition and nondeposition of marine strata in different parts of the world and suggested that sea level rises and falls may be eustatic (global) in origin. Other researchers have since documented the sea level histories of different parts of the world, and some of them have ascribed the apparent synchroneity of these events to episodes of global tectonics (*2, 3*).

Sea level fluctuations have important implications for organic productivity of the oceans and sediment distribution patterns along the continental margins and in the interior basins. Therefore, the study of these fluctuations is of prime interest to hydrocarbon exploration. Sea level changes are also thought to control hydrographic-climatic patterns and, indirectly, biotic distribution patterns as well. Understanding these changes is of considerable value in deciphering past oceanographic (paleoceanographic) conditions.

Developments in seismic stratigraphy during the 1960s and 1970s led to the recognition that primary seismic reflections parallel stratal surfaces and unconformities (*4*). On this basis, Vail *et al*. (*4*) proposed that sediment packages (depositional sequences) bounded by unconformities and their correlative conformities represented

primary units with chronostratigraphic significance. Vail *et al*. used stratal geometries and patterns of onlap, downlap, truncation, and basinward shifts of coastal onlap to interpret sea level histories along various continental margins. The apparent synchroneity of sea level falls in widely separated basins led them to generate a series of charts showing global cycles of relative changes in sea level (*4*).

With the assertion of the method by Vail *et al*. that primary seismic reflections represented time lines, seismic stratigraphy was seen as a breakthrough for regional and global chronostratigraphic correlations. It has been particularly valuable in frontier areas where it aids in the predrill determination of geological exploration parameters from seismic profiles. The original coastal onlap curves (*4*) were largely based on interpretations of seismic sections with paleontological age control from well data. Since publication of the Vail *et al*. method, sea level curves have been a subject of lively debate. The main criticisms of the curves have centered on (i) the lack of adequate corrections for local and regional subsidence and thus the potential error in estimating the magnitude of sea level rises and falls (*5*); (ii) questions about the timing and the global synchroneity of some of the major events and their significance to the events in the deep sea (*5, 6*); (iii) the need for updating the sea level curves in view of the recent refinements of time scales (*6*); and (iv) the nonpublication of supporting evidence (*6,

7), much of which was considered proprietary. Since the original publication, more up-to-date versions of the global coastal onlap curves for the Jurassic and Cenozoic have been published (*8*), and some of the issues mentioned above have been addressed. However, to reduce the dependence on proprietary seismic and well-log data, the need was seen to develop alternative criteria for identifying sea level fluctuations in easily accessible sections, where lessons learned from seismic interpretation of sea level changes could be applied to public domain outcrop data. The recent advances in sequence stratigraphic concepts (*9*) and the development of depositional models of genetically related sediments during various phases of the sea level cycles (*10, 11*) have helped fulfill this need (see Fig. 1).

The sequence-stratigraphic depositional models, together with detailed paleontological data, enhance the ability to recognize genetically related sediment packages in outcrop sections. They also provide independent avenues by which seismic and diverse subsurface data can be augmented and integrated. Sea level rises and falls are manifested by specific physical surfaces that can be used to identify sequences in land-based and offshore marine sections. In this way, sea level changes can be documented in diverse areas that are within the public domain. [Studies listed in (*11*) cover quantitative models, applications in the field, chronostratigraphic basis, and the documentation of this methodology.] These developments represent a major step forward since the first publication of sea level curves (*4*).

Over the past several years stratigraphers at Exxon Production Research (EPR) have attempted to produce a global stratigraphic framework that integrates state-of-the-art magneto-, chrono-, and biostratigraphies with sequences recognized in the subsurface and outcrop sections in different sedimentary basins. These data have provided a new

The authors are on the scientific research staff of Exxon Production Research Company, Houston, TX 77252.

*Present address: Department of Geology, Rice University, Houston, TX 77251.

generation of Mesozoic and Cenozoic cycle charts that go beyond the resolution possible with seismic stratigraphic techniques alone.

In order to publish the new cycle charts (Figs. 2 to 5) without further delay, we have summarized our results in this article. We describe our approach and the results for the Mesozoic (the Triassic, Jurassic, and Cretaceous are dealt with separately here) and the Cenozoic. The sequence-stratigraphic concepts and depositional models have been addressed elsewhere (11).

Chronostratigraphic Basis

The accuracy of a widely applicable correlation framework depends on the reliability of the stratigraphy on which it is based. Our objective has been to build a stratigraphic framework that is advertent to empirical data and is rigorous enough that quick modifications are not necessary as singular new items of data become available. The choice of the linear time scale provides an example of this approach.

Traditional methods of constructing time scales, including some of the more recent attempts, have relied heavily on a few radiometric dates that are used to "nail down" segments of the otherwise extrapolated linear time scale (12). The choice of radiometric dates that are used as "tie points" often depends on an internally justifiable preference of the researchers. The result is that a series of different and equally valid time scales can be constructed on the basis of a differing choice of tie points. Even if the time scale near the fixed tie points is valid, the precision of the rest of the segments will depend on the accuracy of the assumptions used to extrapolate the time intervals. Such assumptions may not always be warranted (13). The tie-point approach is a reasonable option only when reliable radiometric data are extremely sparse, as is still the case for much of the Paleozoic.

Differing time scales can also result from an investigator's preference for a certain type of radiometric technique. Examples are provided by the differing linear scales based exclusively on high-temperature radiometric dates, compared with those based largely on low-temperature dates (14). Although the problems inherent in various radiometric dating techniques are becoming better understood (15), the adoption of one technique to the exclusion of others introduces a distinct bias. It also ignores a large body of
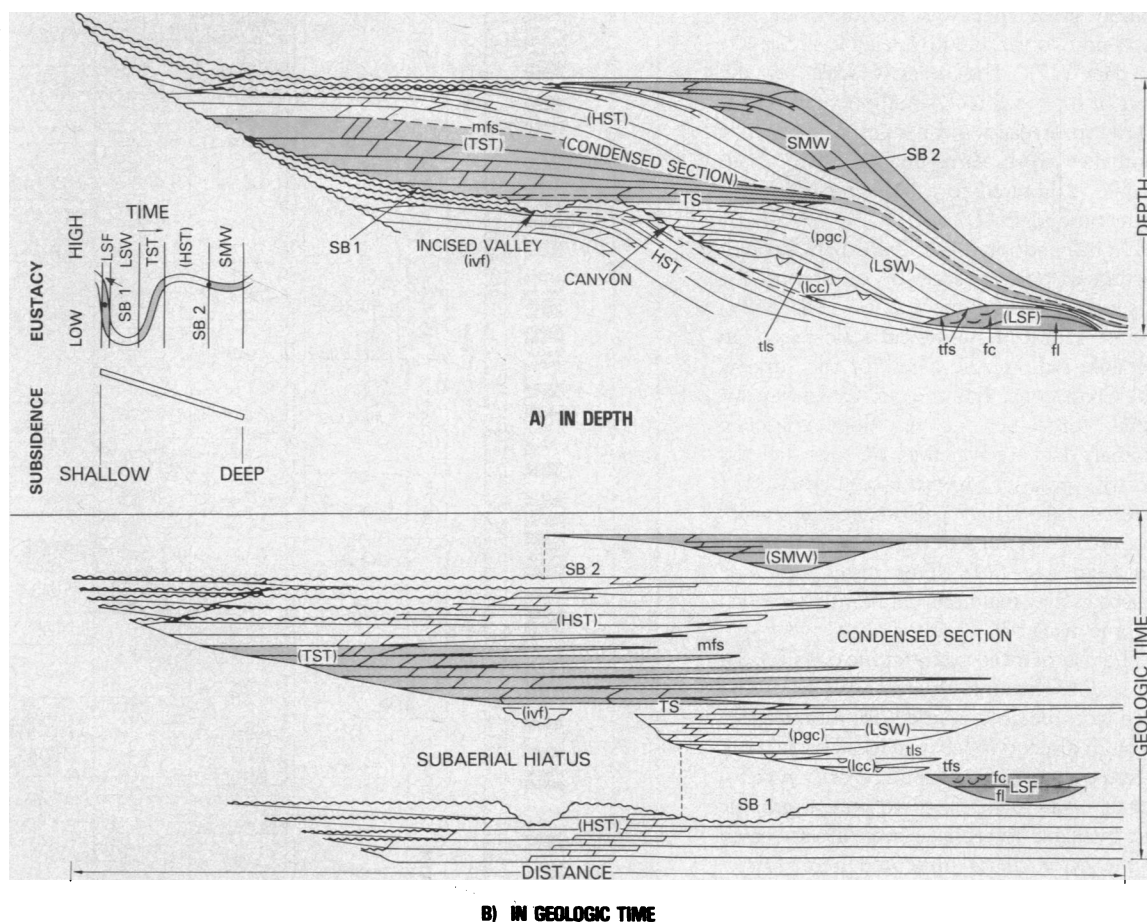
Fig. 1. Sequence-stratigraphic concepts. Depositional model showing systems tracts during the development of type 1 and type 2 sequences that occur after type 1 and type 2 unconformities, respectively. (**A**) The systems tracts in relation to depth. (**B**) The same features plotted against geologic time (legend below this figure explains the symbols).

LEGEND

SURFACES	SYSTEMS TRACTS
(SB) SEQUENCE BOUNDARIES	HST = HIGHSTAND SYSTEMS TRACT
(SB 1) = TYPE 1	TST = TRANSGRESSIVE SYSTEMS TRACT
(SB 2) = TYPE 2	LSW = LOWSTAND WEDGE SYSTEMS TRACT
(DLS) DOWNLAP SURFACES	ivf = incised valley fill
(mfs) = maximum flooding surface	pgc = prograding complex
(tfs) = top fan surface	lcc = leveed channel complex
(tls) = top leveed channel surface	LSF = LOWSTAND FAN SYSTEMS TRACT
(TS) TRANSGRESSIVE SURFACE	fc = fan channels
(First flooding surface above maximum regression)	fl = fan lobes
	SMW = SHELF MARGIN WEDGE SYSTEMS TRACT

potentially valuable analytical and empirical data.

To produce a practical time scale with the widest possible use, one must reconcile all reliable observations. Our linear scales, as shown on the Mesozoic and Cenozoic cycle charts, are best-fit solutions of the analytically sound and stratigraphically constrained radiometric dates (16). We believe a solution that does not overlook any potentially useful chronological information generates time scales that are more stable and utilitarian and that will resist the need for quick modifications.

The magnetostratigraphy (geomagnetic polarity reversals) adopted for the cycle charts is a combination of four different types of paleomagnetic information of varying quality. We have adopted a polarity scale of geomagnetic reversals of the past 6.5 million years that was identified in lava flows and constrained by reliable radiometric data (17). The polarity scale for the interval from 6.5 to 84 million years ago is based on stacked mean ages of magnetic anomalies from three major ocean basin profiles, calibrated to a best-fit radiometric linear time scale (18).
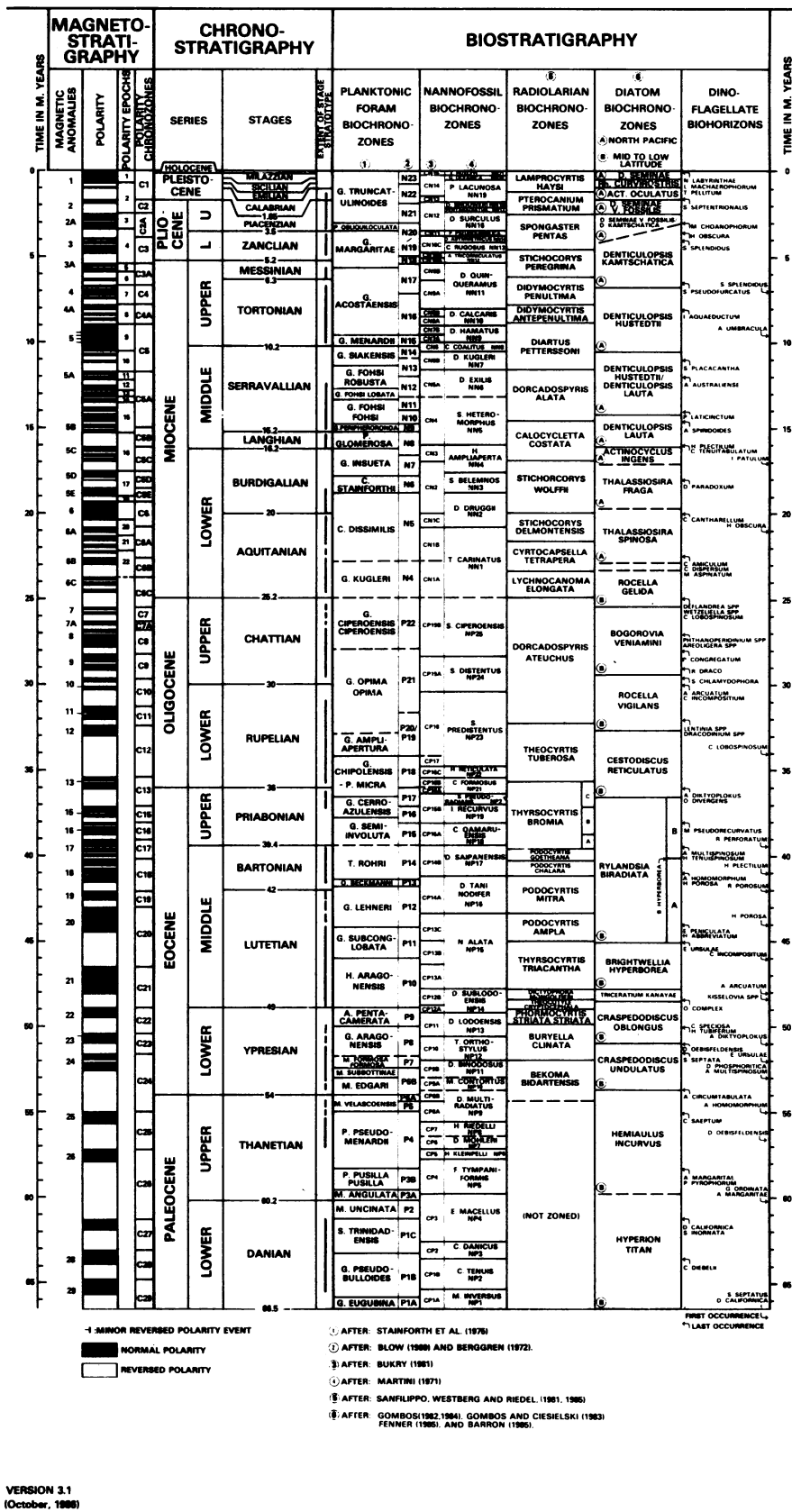
We have adopted the Oxfordian through Barremian polarity scale by calibrating the M-series magnetic anomalies (M0–M29) against a best-fit numerical scale based on available radiometric dates for the Jurassic and Cretaceous. For the pre-Oxfordian interval, for which no sea floor magnetic anomaly data are available, we constructed a tentative polarity reversal model based on a synthesis of various paleomagnetic studies on outcrop sections of the Triassic through Callovian age (19). This model may be revised as new magnetic data for this interval become available.

The magnetobiostratigraphic basis for the Cretaceous through Quaternary interval has been considerably refined in recent years through direct ties between fossil occurrence datum events and magnetic polarity reversal events. All such magnetobiostratigraphic data available to us have been incorporated in the cycle charts presented here. Direct

correlations between reversals and biohorizons (first and last occurrences of calcareous plankton) in the tropical to temperate regions are now available for much of the Cenozoic and late Cretaceous (20). For

parts of the Neogene, such ties are also available for siliceous plankton (21, 22). But for the Jurassic and early Cretaceous, such first-order correlations between polarity reversal events and fossil occurrences are limit-

Fig. 2. Cenozoic chronostratigraphy and cycles of sea level change. The linear time scale (in million years before present) is repeated on the left, center, and right of the cycle chart. Sections include magnetostratigraphy, chronostratigraphic subdivisions, biostratigraphy, and sequence stratigraphy. Long- and short-term eustatic curves complete the chart. The key at the bottom of the figure explains the relative magnitude of sequence boundaries (type 1 and 2 boundaries are distinguished) and condensed sections. Sources (citations in the figure) for the Cenozoic magnetostratigraphy are listed in (17, 18) and for biostratigraphy in (31). (Two halves of the figure are reproduced on facing pages.)

ed to a few isolated studies (23).

Much work needs to be done on the Mesozoic sections before a clear picture of the relation between polarity reversal sequences and fossil zones can emerge. Until that time, we must assign equal durations to the subdivisions of such commonly used zonal schemes as those based on ammonites within individual stages of much of the Jurassic and Lower Cretaceous.

SEQUENCE STRATIGRAPHY / EUSTATIC CURVES chart. Authors: B.U. HAQ, J. HARDENBOL, P.R. VAIL, R.C. WRIGHT, L.E. STOVER, G. BAUM, T. LOUTIT, A. GOMBOS, T. DAVIES, C. PFLUM, K. ROMINE, H. POSAMENTIER
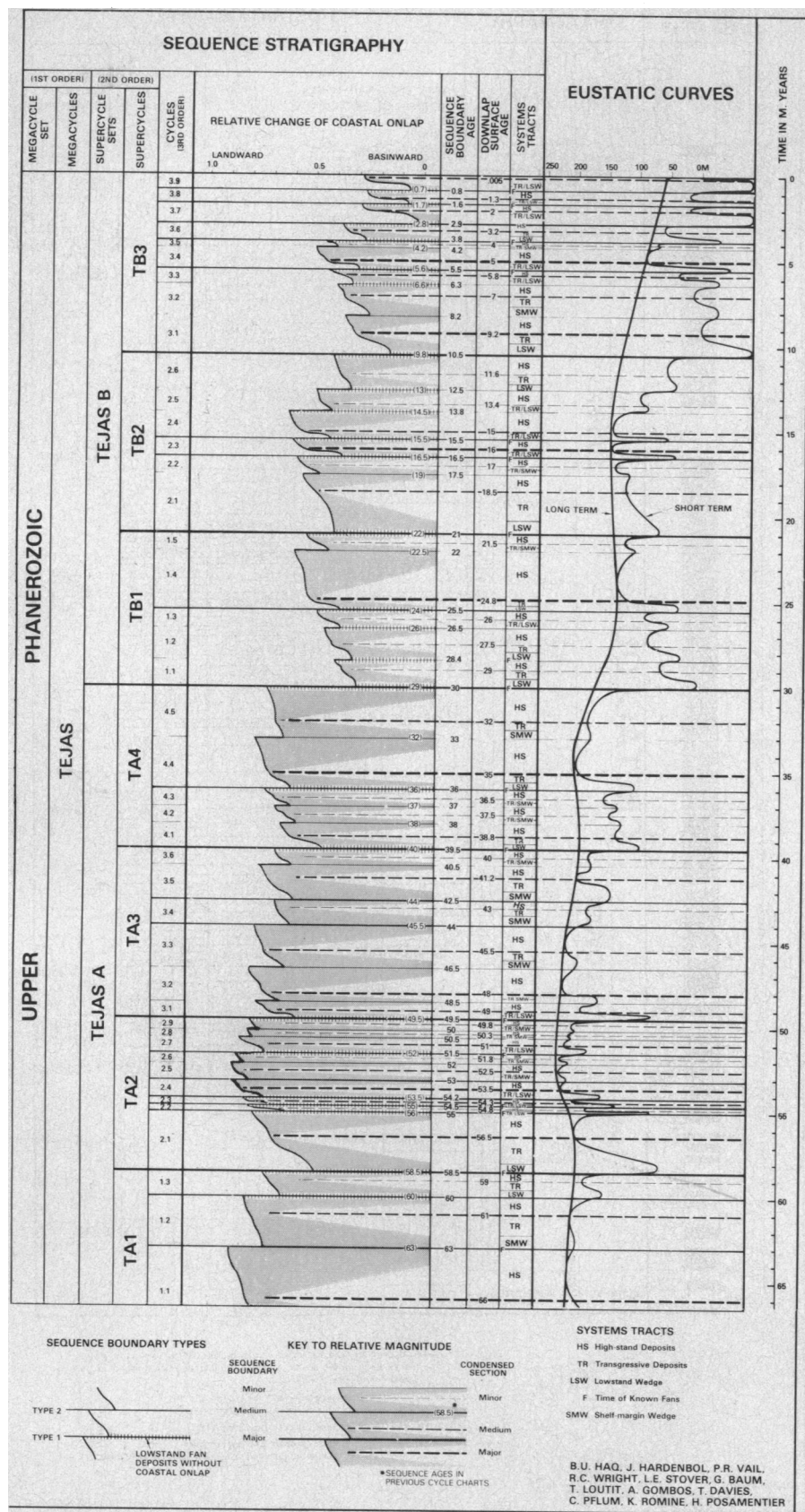
By tradition, the European stages of the Mesozoic and Cenozoic have come to be accepted as the basic units of chronostratigraphy for worldwide correlations. We correlated these stages with our linear scale and magnetobiostratigraphy by establishing the sequence-stratigraphic framework of the stage stratotypes and other key reference sections from various parts of the world. The standard stages could then be integrated more accurately into the cycle charts through the biostratigraphic and physical-stratigraphic relations of the stratotypes. A typical example of the sequence-stratigraphic approach is provided by the Chattian Stage of the Upper Oligocene.

The neostratotype of the Chattian at Doberg bei Bünde in West Germany consists of about 70 m of nearshore to offshore marine sands and marls (24). The litho- and biofacies, grain-size analysis, and paleoenvironmental considerations suggest that two distinct depositional sequences separated by an unconformity are present. The lower sequence consists of fining-upward and deepening transgressive deposits that are overlain by coarser highstand, nearshore to littoral, deposits. This succession of depositional packages is repeated in the upper sequence, although in a somewhat deeper setting. The biostratigraphic data permit a precise correlation of the neostratotype to two of the Upper Oligocene sequences (TB1.2 and 1.3, Fig. 2) on the cycle chart. Such sequence-stratigraphic studies of the stage stratotypes have helped us to position the stages more accurately within the standard chronostratigraphic framework.

Documentation of Sea Level Changes Since the Triassic

The new generation of cycle charts of sea level fluctuations is largely based on the study of sequences in outcrops that augments the results from subsurface (seismic and well-log) data. These cycle charts are an improvement over previously published ones, which were based entirely on subsurface information. The documentation of the Mesozoic and Cenozoic sequences is derived from outcrop sections in various parts of the world. Much of this documentation, however, comes from marine outcrops spread throughout central and western Europe, and in the United States, along the Gulf and Atlantic coasts and in the western interior (Colorado, Utah, and Wyoming). All of these sections are within the public domain where the results can be studied and tested (25–28).

Ideally, sequence-stratigraphic analysis (recognition of depositional sequences relat-

ed to sea level rises and falls) should be carried out on seismic sections and well logs from an area, in combination with extensive outcrop studies of the same region. These data can be integrated to establish an accurate chronostratigraphic framework and to identify depositional sequence boundaries through litho- and biofacies analyses. In practice, however, all three types of data are usually not available for all areas.

Changes of relative sea level, which is the combined effect of subsidence and eustacy, control the accommodation potential of the sediments and the distribution of facies within the system tracts. The details of the sequence-stratigraphic concepts and the criteria used to identify depositional systems tracts (Fig. 1) in outcrops have been dealt with elsewhere (11). In marine outcrops three depositional surfaces (systems-tracts boundaries) can usually be identified. The most readily identifiable surface is the "transgressive surface" (Fig. 1), which occurs above the lowstand deposits that are characterized by sediments of the maximum regressive phase. The transgressive surface heralds the onset of a relatively rapid sea level rise and marked lithologic changes associated with the rise. In the absence of lowstand deposits, the transgressive surface may coincide with the underlying unconformable portion of the sequence boundary.

The second most easily recognizable surface in outcrops is the surface of maximum flooding, which is referred to as the "downlap surface" on seismic profiles (Fig. 1). This surface is associated with the condensed section that occurs within the transgressive and highstand systems tracts. It depicts an interval of depositional starvation when the rapidly rising sea level moves the sediment depocenters landward. Because of the lack of terrigenous input, the condensed section may be expressed as a zone of high pelagic fossil concentration, or as hardground caused by lithification. The relative duration of slow sedimentation represented by the condensed section increases basinward until, beyond the areas of terrigenous influence, the deposition in the deeper basin is theoretically a series of stacked condensed sections. The marked lithologic and faunal changes across the condensed section can also be mistaken for the sequence boundary.

The third recognizable depositional surface in outcrops is the sequence boundary. In seismic sections this is expressed by the

downward (basinward) shift of coastal onlap. In outcrops the sequence boundary may be represented by an obvious unconformity or by more subtle changes, depending on the position of the section along the shelf-to-basin profile and on the rate of relative sea level fall. For example, if the location of the section is more shoreward along the
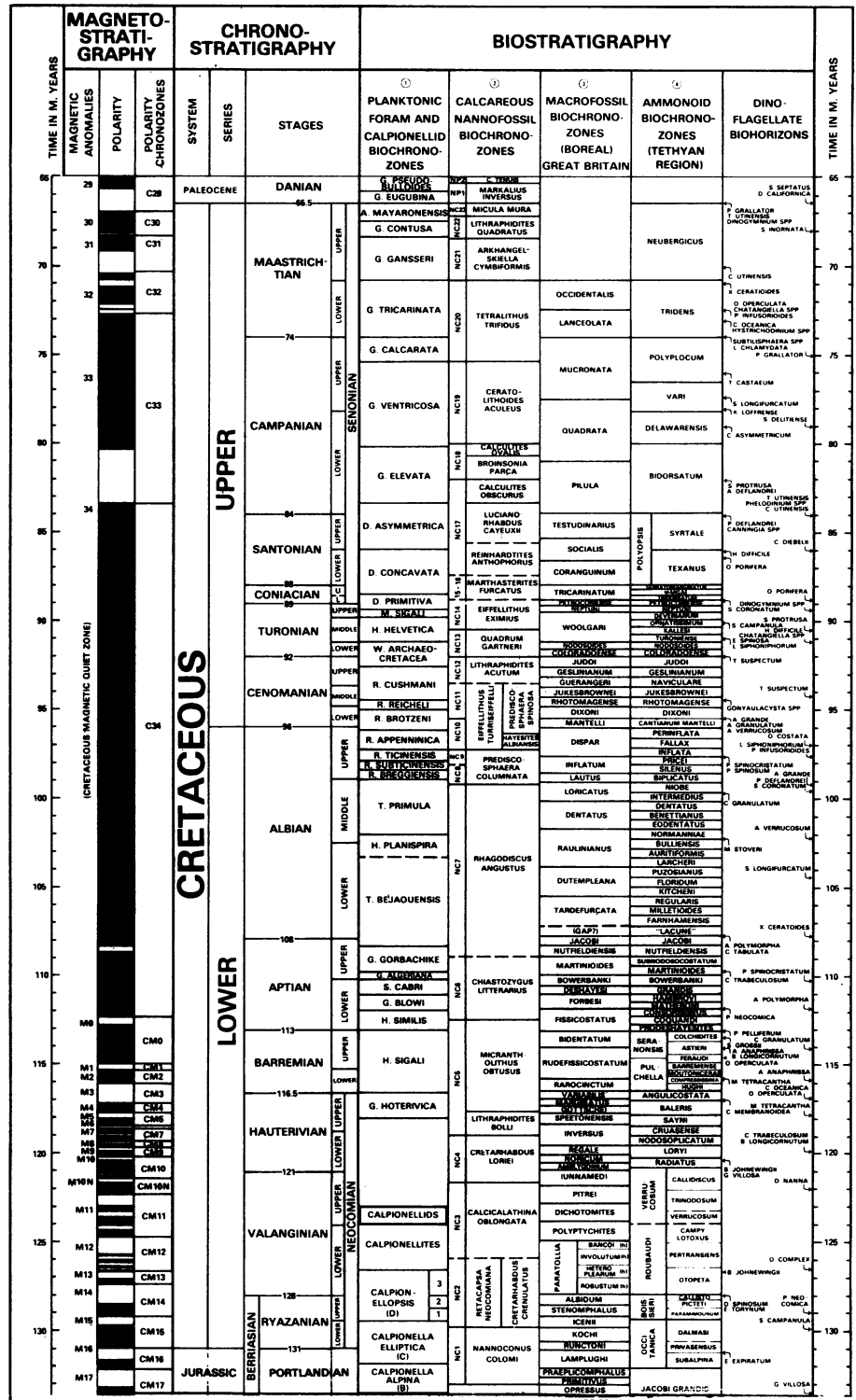

Fig. 3. Cretaceous chronostratigraphy and cycles of sea level fluctuation (see Fig. 2 and caption for key and explanation). Sources for Cretaceous magnetostratigraphy are listed in (18) and for biostratigraphy in (33). (Two halves of the figure are reproduced on facing pages.)

shelf, the probability of deposition of low-stand deposits is reduced. If located updip, the deposition of such deposits may be entirely precluded, so that the sequence boundary is an unconformity that may coincide with the transgressive surface. Downdip, the sequence boundary becomes conformable and occurs within the overall shoaling-upward sediments. It is typically characterized by a change from interbedded progradational deposits to more massive aggradational deposits.

Similarly, significant falls of sea level are manifested by prominent unconformities with erosional truncation caused by subaerial exposure. Type 1 unconformities (Fig. 1) produced as a result of rapid sea level falls that are greater than subsidence at the shelf edge may expose the entire shelf. The sea withdrawal below the shelf edge also signals the development of incised valley systems on the shelf that may be accompanied by lowstand fan (lowstand fan systems tract) deposition offshore if a source of sand is available. The incised river system feeds the fan directly, and the fan deposits therefore do not show coastal onlap (Fig. 1).

As soon as the regional subsidence begins to outstrip the slowing rate of sea level fall, relative sea level begins to rise, and backfilling of the incised valleys commences. The lowstand facies (lowstand wedge systems tract) accumulate between the shelf edge and the fan; these deposits may initially develop a leveed channel complex. Eventually, lowstand deposits prograde over the leveed channel complex and the fan deposits, as the shoreline reaches its maximum basinward regression. As the global sea level begins to rise, the transgression of the shelf is marked by the transgressive surface, and the landward back-stepping transgressive facies (transgressive systems tract) begin to be deposited. The transgressive deposits are in turn overlain by the prograding highstand deposits (highstand systems tract) during the highstand phase. Short-term, higher frequency flooding events occur in all systems tracts and have been termed parasequences or pacs (29) (Fig. 1).

When the rate of sea level fall is slow, the withdrawal of the sea is more deliberate, and the whole shelf may not be exposed. The resulting unconformity is less prominent (type 2 unconformity). In this case the lowstand fan and the leveed-channel deposits do not develop. Instead, the shelf margin facies (shelf margin wedge systems tract) prograde directly over the shelf edge and onto the slope (Fig. 1).

The application of sequence-stratigraphic concepts (11) to outcrop sections has provided the framework to identify and classify major, medium, and minor sequences. In practice, only sequences of major and medium magnitude are discernible at the regional seismic level. Minor sequences are generally beyond the resolution obtainable with seismic data alone, but they can be mapped by detailed well-log studies and in outcrop sections.

We list here the only major areas and
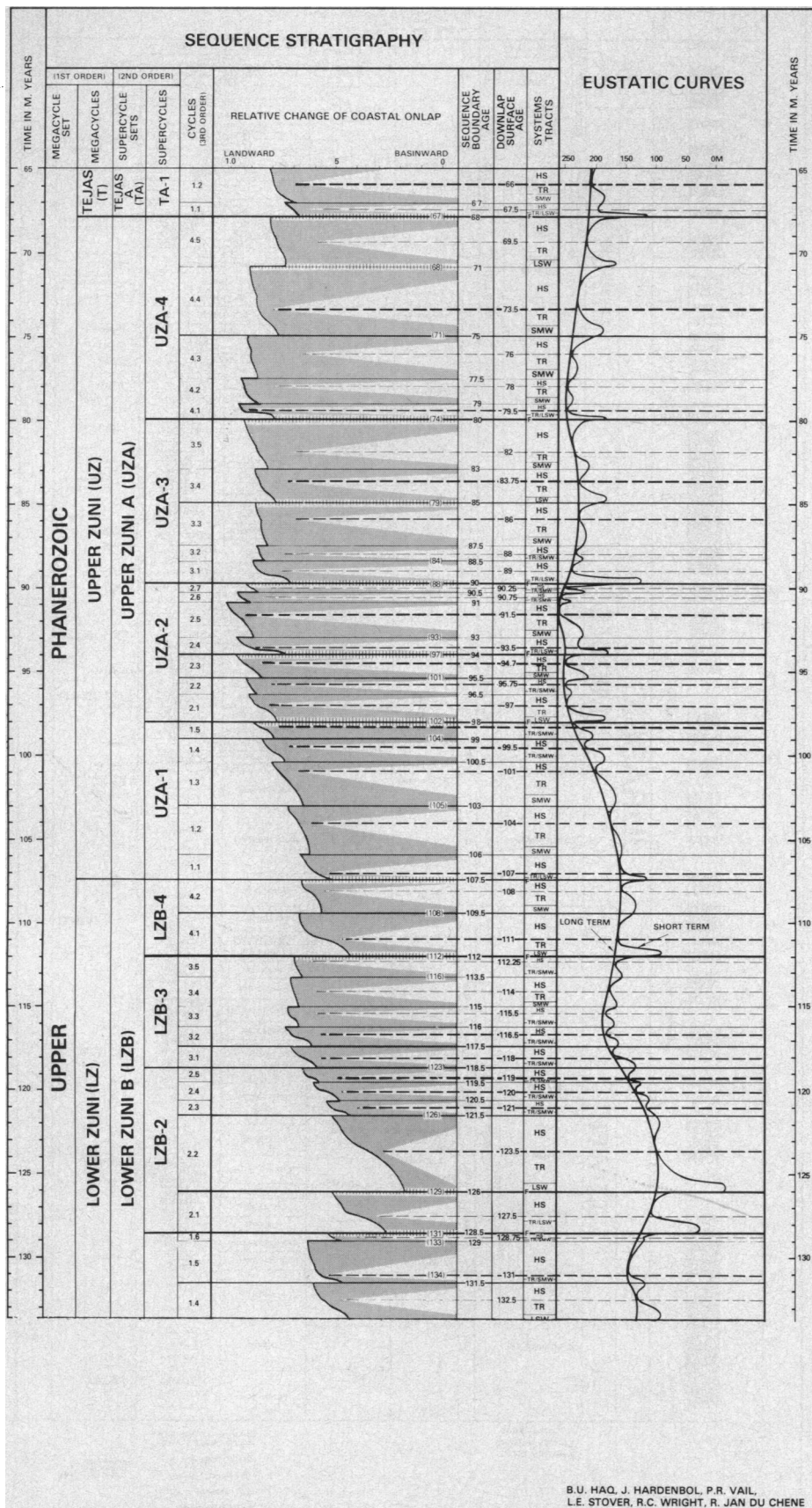
sections that were used for our documentation. Study areas for the Cenozoic (25), Cretaceous (26), Jurassic (27), and Triassic (28) are listed separately.
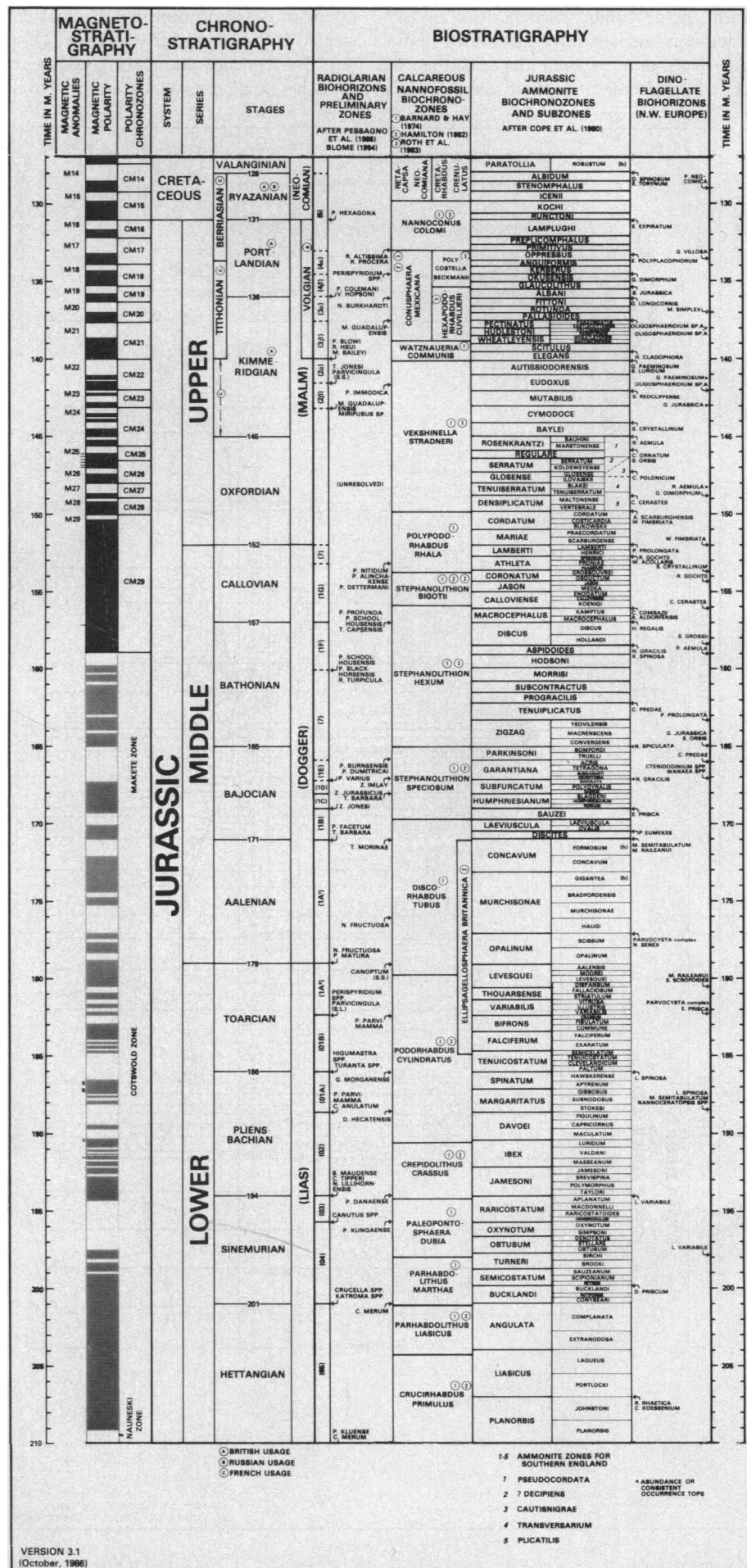
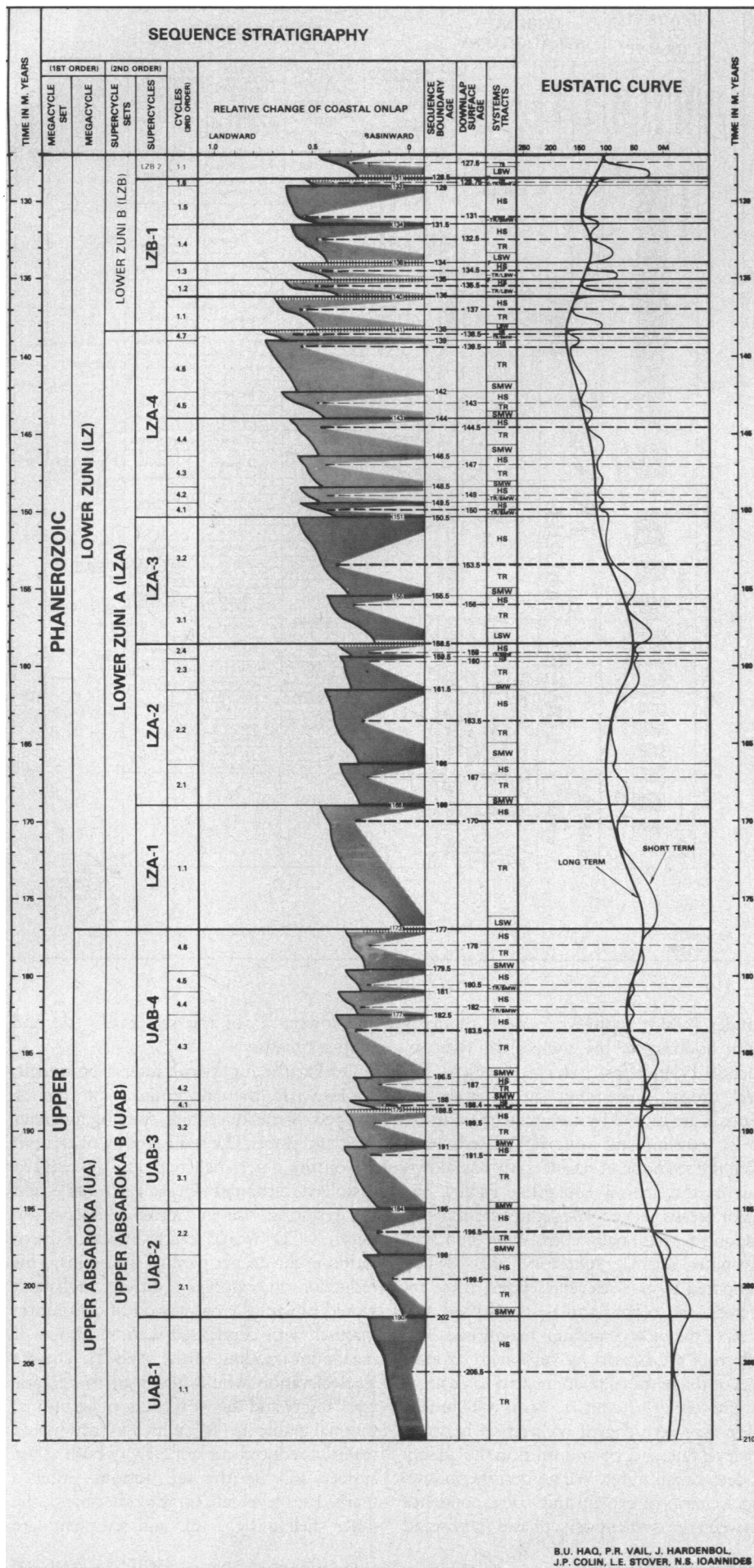## Results and Description of the Cycle Charts

A series of four cycle charts depict the chronology of sea level fluctuations in the Cenozoic, Cretaceous, Jurassic, and Triassic and cover the eustatic history of the last 250 million years (Figs. 2 through 5). On each cycle chart the linear time scale in million years before present is repeated in three places. The cycle charts incorporate a vast combination of information that helps to chronicle the sea level changes in a precise manner. This information is presented in five sections. The first section is magnetostratigraphy. Both the sea floor magnetic anomaly data, where available, and polarity reversal sequence are included (17–19).

The second section includes chronostratigraphy. The columns contain the system, series, and stage designations (for the Cenozoic, series and stage only). We have adopted the commonly used western European stages that have come to be accepted as standard international chronostratigraphic units. Some of the suprastage chronostratigraphic designations (such as Lias, Dogger, and Malm for the Jurassic, Fig. 4) that are still frequently used in some regions are also indicated within the stage column (30).

The third section depicts biostratigraphy and includes two types of information. Formally defined zonal schemes (based on first or last occurrence of fossil taxa or their total ranges) are included. They differ, however, for the Cenozoic (31), Cretaceous (32, 33), Jurassic (34), and Triassic (35), depending on the relative usefulness of the groups for subdividing the particular stratigraphic interval. The second type of information in these columns is the first and last occurrence events, or biohorizons, of those fossil groups whose zonal schemes have not yet been formally established or become widely accepted (for example, the dinoflagellate biohorizons for the Cenozoic through the

Fig. 4. Jurassic chronostratigraphy and cycles of sea level fluctuation (see Fig. 2 and caption for key and explanation). Sources for Jurassic magnetostratigraphy are listed in (18, 19), and for biostratigraphy in (34). The synthesized pre-Callovian (older than 160 million years) magnetic polarity reversals model (shown in gray and white) may be subject to modification when additional magnetic data become available. (Two halves of the figure are reproduced on facing pages.)

SEQUENCE STRATIGRAPHY

EUSTATIC CURVE

TIME IN M. YEARS

(1ST ORDER) MEGACYCLE SET — (2ND ORDER) MEGACYCLE — SUPERCYCLE SETS — SUPERCYCLES — CYCLES (3RD ORDER)

RELATIVE CHANGE OF COASTAL ONLAP
LANDWARD 1.0 ... 0.5 ... BASINWARD 0

SEQUENCE BOUNDARY AGE — DOWNLAP SURFACE AGE — SYSTEMS TRACTS

LONG TERM — SHORT TERM

PHANEROZOIC — LOWER ZUNI (LZ) — UPPER

LOWER ZUNI B (LZB) — LZB-1 — LOWER ZUNI A (LZA) — LZA-4 — LZA-3 — LZA-2 — LZA-1

UPPER ABSAROKA (UA) — UPPER ABSAROKA B (UAB) — UAB-4 — UAB-3 — UAB-2 — UAB-1

B.U. HAQ, P.R. VAIL, J. HARDENBOL,
J.P. COLIN, L.E. STOVER, N.S. IOANNIDES

Jurassic, and the radiolarians for Jurassic and Triassic). Much of this information should be regarded as preliminary until future work confirms the correlation of these events with the global chronostratigraphic framework. The dinoflagellate occurrences, in particular, largely from western European sections, represent an aggregate of the data of EPR palynologists (36) and will need to be corroborated elsewhere before they can be applied on a wider basis.

The fourth section contains the terminology for sequence stratigraphy. It includes sequence chronozones or cycles (megacycles, supercycles, and cycles) (37) and scaled relative changes of coastal onlap. The ages of the cycle boundaries and downlap surfaces are indicated in separate columns, as are the depositional systems tracts (boundaries where fans have been observed are indicated by "F" in this column, Figs. 2 through 4). Major, medium, and minor sequence boundaries and condensed sections are identified by the relative thickness of the lines drawn through them (38). The unshaded triangles within each coastal onlap cycle represent the condensed sections, depicting the intervals of slow deposition after rapid sea level rise, the relative duration of which increases basinward.

The long- and short-term eustatic curves are plotted in the last section. The scale (in meters) represents the best estimate of sea level rises and falls compared with the present-day mondial mean sea level (39).

In the long term, the generally low sea levels of the late Paleozoic (Pennsylvanian and Permian), which reached their lowest point in the Tatarian, continued into the Triassic and early Jurassic. In the Hettangian, the sea level dipped to another markedly low position; the levels remained generally low through much of the middle Jurassic, rising somewhat in the Bajocian, but falling again in the late Bathonian. The trend reversed itself in the Callovian, and the long-term sea level continued to rise through the Oxfordian, reaching a Jurassic peak in the Kimmeridgian.

After a transient but marked decline in the early Valanginian, the sea level began to rise rapidly, remaining high through the remainder of the Cretaceous. It reached its Mesozoic-Cenozoic peak in the early Turonian time. After this mid-Cretaceous high, a gradual decline of sea level began in the latest Cretaceous and continued through the Cenozoic. With the exception of relatively higher levels in the Danian, Ypresian, Rupelian, Langhian through early Serravallian, and Zanclian, this trend toward lower sea levels continues to the present time.

In the short term, the major sea level falls occurred at the base of Portlandian, in early

Fig. 5. Triassic chronostratigraphy and cycles of sea level change (see Fig. 2 and caption for key and explanation). Sources for the synthesized Triassic and early-middle Jurassic magnetic polarity reversal model are listed in (19). This model may be subject to future modifications. Sources for Triassic biostratigraphy are in (35). (Two halves of the figure are reproduced on facing pages.)
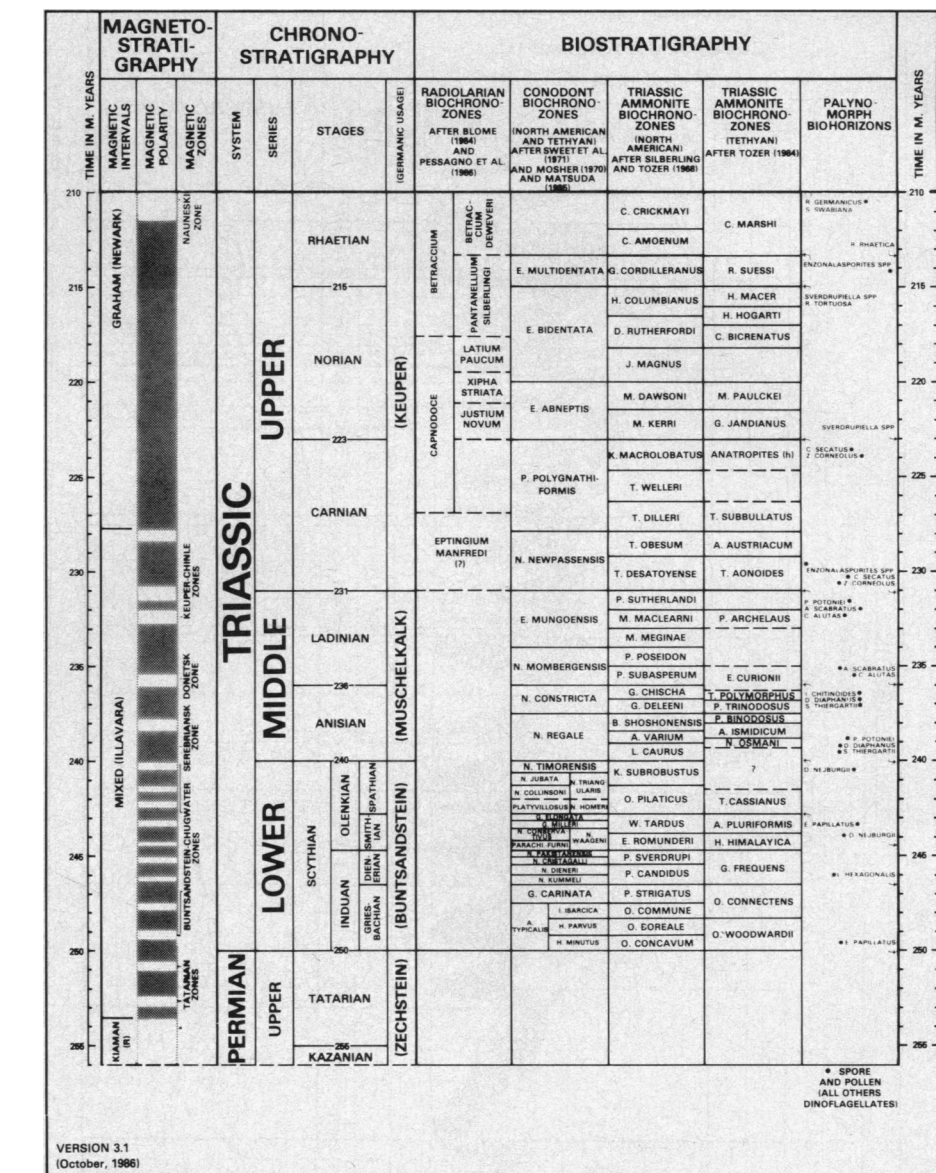
Aptian, mid-Cenomanian, late Turonian, late Maastrichtian, early Thanetian, latest Ypresian, latest Bartonian, near the Rupelian-Chattian boundary, in Burdigalian-Langhian, in the late Serravallian, and throughout the late Pliocene-Pleistocene interval. These short-term, but marked, sea level falls are frequently associated with worldwide major unconformities. At least since the Oligocene, sea level drops may be in large part due to the increasing influence of glaciation. This influence is manifested by the relatively large variations in amplitude of the short-term sea levels since the mid-Oligocene.

A total of 119 Triassic through Quaternary sea level cycles have been identified in the new generation Mesozoic-Cenozoic cycle charts. Of these, 19 began with major sequence boundaries, 42 began with relatively medium magnitude sequence boundaries, and 58 were represented by minor sequence boundaries. As mentioned earlier, only the sequence boundaries of major and medium magnitude can be identified generally at regional seismic level. Detailed well-log or outcrop studies are usually necessary to resolve the minor sequences.

Conclusions

We have described our approach in chronicling the Mesozoic and Cenozoic history of sea level fluctuations from various parts of the world. Our objective has been to make the cycle charts public in the most expedient manner possible. In this article we have not attempted to address the important issues of the causes of sea level change, the absolute magnitude of the sea level rises and falls through time, the implication of these changes for the continental margin and deep-sea sedimentary budgets, or their influence on hydrography, climate, and biotic distribution and evolution.
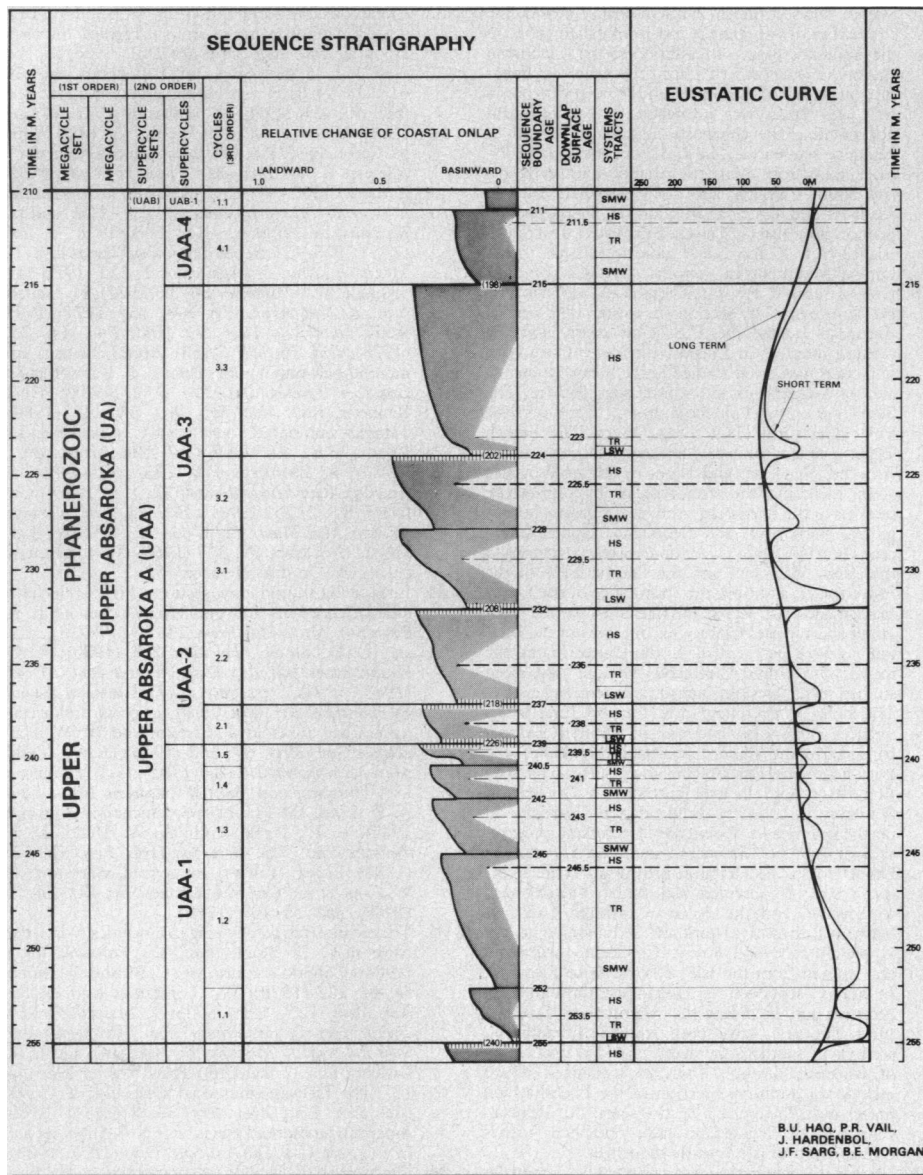
A cursory comparison, for example, could not establish a clear relation between oceanic sedimentation rates (40) and sea level fluctuations. A comparison of Neogene sea level cycles with known intervals of widespread gaps in deep-sea sedimentation (41) reveals, however, that these gaps are coincident either with the downlap surfaces (condensed sections) of major and medium magnitudes (which represent periods of maximum flooding of the shelves) or with sequence boundaries (which represent sea level drops), depending on whether the hiatuses are caused by carbonate dissolution or by erosion and removal of sediments from the sea floor. A recent study has shown that in the central equatorial Pacific, the major breaks in Neogene sedimentation correspond to regionally correlatable and synchronous seismic reflectors (42). When compared to our sea level cycles, these reflectors also correspond to condensed sections of major and medium magnitude. The reflectors are caused by carbonate dissolution or diagenesis and are related to changes in the ocean chemistry (42). Obviously, there may be a cogent connection between sea level fluctuations and shifts in the quality of deep ocean water. We suggest the following scenario to explain this correspondence between the two opposite phases (highstand and lowstand) of the sea level cycle and deep-sea hiatuses.

During the highstand, after a prominent sea level rise, the terrigenous sediments are trapped on the inner shelf, starving the outer shelf and slope. The sequestering of carbonate on the inner shelf may lead to reduced dissolved carbonate in seawater (43), and the resulting rise in calcite compensation depth (CCD) would lead to increased dissolution in the deeper parts of the basins. This reduction in carbonate during highstand would explain the correlation of dissolution hiatuses with condensed sections (times of maximum flooding of the shelves). The sea level elevation would also lead to climatic equitability and the weakening of latitudinal thermal gradients (44), which in turn would result in reduced current activity both at the surface and on the sea bottom. After a marked sea level fall, on the other hand, the inner shelf is bypassed, and sediments are

1164

deposited during the different phases (lowstand, transgressive, and highstand) of sea level cycles [see R. M. Mitchum, P. R. Vail, J. B. Sangree, *Am. Assoc. Pet. Geol. Mem.* 26, 117 (1977)].

directly transported to the outer shelf or slope. The resulting increase in carbonate content of the seawater and the lowering of CCD would reduce carbonate dissolution. But the climatic inequitability and strengthened thermal gradients during the lowstand (44) would lead to intensified circulation and increased bottom water activity, causing widespread erosion on the sea floor. This process explains the correspondence of the erosional hiatuses to sequence boundaries.

REFERENCES AND NOTES

1. E. Suess, *The Face of the Earth* (Clarendon, Oxford, 1906), vol. 2, p. 535.
2. H. Stille, *Grundfragen der vergleichenden Tektonik* (Borntraeger, Berlin, 1924); A. W. Grabau, *Oscillations or Pulsations* (16th International Geological Congress, Washington, DC, 1933); L. L. Sloss, *24th Int. Geol. Congr.* 6, 24 (1972).
3. L. L. Sloss, *Geol. Soc. Am. Bull.* 74, 93 (1963).
4. P. R. Vail *et al.*, *Am. Assoc. Pet. Geol. Mem.* 26, 49–212 (1977).
5. W. C. Pitman III, *Geol. Soc. Am. Bull.* 89, 1389 (1978); G. Bond, *Geology* 6, 247 (1978); A. B. Watts and M. S. Steckler, in *Deep Sea Drilling in the Atlantic Ocean: Continental Margins and Paleoenvironment*, M. Talwani, W. Hay, W. B. F. Ryan, Eds. (American Geophysical Union, Washington, DC, 1979), Maurice Ewing Series, vol. 3, pp. 218–239; A. B. Watts, *Nature (London)* 297, 469 (1982); A. W. Bally, *Am. Geophys. Union Geodynamics Ser.* 1, 5 (1980).
6. N.-A. Mörner, *Geology* 9, 344 (1981); N. Parkinson and C. P. Summerhayes, *Am. Assoc. Pet. Geol. Bull.* 69, 685 (1985); A. D. Miall, *ibid.* 70, 131 (1986); B. E. Tucholke, *Soc. Econ. Paleontol. Mineral. Spec. Publ.* 32, 23 (1981).
7. A. Hallam, *Annu. Rev. Earth Planet. Sci.* 12, 205 (1984); A. D. Miall, in (6).
8. P. R. Vail and J. Hardenbol, *Oceanus* 22, 71 (1979); P. R. Vail and R. G. Todd, in *Petroleum Geology of the Continental Shelf of Northwest Europe*, L. V. Illing and G. D. Hobson, Eds. (Institute of Petroleum Geology, London, 1981), pp. 216–235; P. R. Vail, J. Hardenbol, R. G. Todd, *Am. Assoc. Pet. Geol. Mem.* 36, 129 (1984).
9. Sequence is a widely used term in earth science, but here sequence refers specifically to the depositional sequence or the succession of sediments deposited during a complete sea level cycle, that is, from a sea level fall to subsequent rise and ending with the next fall (Fig. 1). Sequence stratigraphy is broadly defined as the branch of stratigraphy that deals with depositional sequences of genetically related strata
10. Various authors in C. Wilgus *et al.*, Eds., "Sea level change—an integrated approach," *Soc. Econ. Paleontol. Mineral. Spec. Publ.*, in press.
11. In addition to the references in (8), sequence-stratigraphic concepts, methodology, and chronostratigraphic basis have also been presented in the following: J. Hardenbol *et al.*, *2nd Int. Conf. Paleoceanogr.* (abstr.) (1985), p. 40; B. U. Haq *et al.*, *ibid.* (abstr.), p. 40; T. S. Loutit *et al.*, *ibid.* (abstr.), p. 52; T. C. Moore *et al.*, *ibid.* (abstr.), p. 55; B. U. Haq *et al.*, *Soc. Econ. Paleontol. Mineral.* (abstr.) (1986), p. 121; *Geol. Soc. Am. Abstr. Programs* (1986), p. 628. Details of quantitative models and theoretical concepts of sequence stratigraphy appear in M. T. Jervey, in (10); H. Posamentier, M. T. Jervey, P. R. Vail, *ibid.*; J. van Wagoner, *ibid.* Examples of applications of these concepts in the field are included in P. R. Vail *et al.*, *Bull. Soc. Geol. France*, in press; S. M. Greenlee, F. W. Schroeder, P. R. Vail, in *North American Continental Margins*, R. Sheridan and J. Grow, Eds. (commemorative volumes, Decade of North American Geology, Boulder, CO), in press; G. R. Baum, in (10); J. F. Sarg, *ibid.*; T. Loutit, J. Hardenbol, P. R. Vail, *ibid.* Details of the chronostratigraphic basis appear in B. U. Haq, J. Hardenbol, P. R. Vail, *ibid.*
12. For example, W. A. Berggren, *Lethaia* 5, 195 (1972); J. Hardenbol and W. A. Berggren, *Am. Assoc. Pet. Geol. Spec. Studies* 6, 213 (1978); W. A. Berggren, D. V. Kent, J. J. Flynn, J. A. Van Couvering, *Geol. Soc. Am. Bull.* 96, 1418 (1985); W. B. Harland *et al.*, *A Geologic Time Scale* (Cambridge Univ. Press, Cambridge, 1982).
13. Time scales are commonly extrapolated between fixed points, assuming constant sedimentation or sea floor spreading rates.
14. Compare, for example, the Paleogene time scale based largely on low-temperature radiometric dates (K/Ar dates on glauconites) [G. S. Odin *et al.*, in *Numerical Dating in Stratigraphy*, G. S. Odin, Ed. (Wiley-Interscience, New York, 1982), part 2, pp. 957–960], with one based exclusively on selected high-temperature dates (K/Ar dates on bentonites) [W. A. Berggren, D. V. Kent, J. J. Flynn, J. A. Van Couvering, *Geol. Soc. Am. Bull.* 96, 1407 (1985)].
15. Various authors in G. S. Odin, Ed., *Numerical Dating in Stratigraphy* (Wiley-Interscience, New York, 1982), part 1, pp. 151–454.
16. In constructing the linear time scale, we used both high- and low-temperature radiometric dates. Criteria for the selection of radiometric dates have been that they be analytically acceptable and stratigraphically constrained. When reliable low- and high-temperature dates are available for the same stratigraphic interval (for example, the Aptian through Maastrichtian), the older ranges of the low-temperature dates show significant overlap with the younger ranges of the high-temperature dates.
17. I. McDougall, N. D. Watkins, G. P. Walker, L. Kristjansson, *J. Geophys. Res.* 81, 1501 (1976); I. McDougall, K. Saemundsson, H. Johannesson, N. A. Watkins, L. Kristjansson, *Geol. Soc. Am. Bull.* 88, 1 (1977); E. A. Mankinen and G. B. Dalrymple, *J. Geophys. Res.* 84, 615 (1979). (If not already converted, we have converted all radiometric dates according to new decay constants.)
18. Composite late Cretaceous–Cenozoic polarity reversal scales have been developed from the marine magnetic anomaly scale of J. R. Heirtzler *et al.* [*J. Geophys. Res.* 73, 2119 (1968)], with later refinements by J. L. LaBrecque, D. V. Kent, and S. C. Cande [*Geology* 5, 330 (1977)] and W. Lowrie and W. Alvarez [*ibid.* 9, 392 (1981)]. The Callovian (late Jurassic) through Cretaceous polarity reversal scales have developed from magnetic anomaly profiles of R. L. Larson and W. C. Pitman III [*Geol. Soc. Am. Bull.* 83, 3645 (1972)], R. L. Larson and T. W. C. Hilde [*J. Geophys. Res.* 80, 2586 (1975)], and S. C. Cande, R. L. Larson, and J. L. LaBrecque [*Earth Planet. Sci. Lett.* 41, 434 (1978)]. To arrive at the late Cretaceous–Cenozoic stacked mean ages for the magnetic anomalies (anomalies 34 through 1), we used the following sea floor anomaly profiles from the North Pacific: W. C. Pitman III, E. M. Herron, J. R. Heirtzler, *J. Geophys. Res.* 73, 2969 (1968); for the South Pacific: *ibid.*, p. 2069; and for the South Atlantic: G. O. Dickson, W. C. Pitman III, J. R. Heirtzler, *ibid.*, p. 2987. Magnetic chron nomenclature (polarity chronozones) for the late Cretaceous–Cenozoic is largely by L. Tauxe *et al.* [*Palaeogeogr.*

Figure (Sequence Stratigraphy / Eustatic Curve chart)

SEQUENCE STRATIGRAPHY — EUSTATIC CURVE

Headers: TIME IN M. YEARS | MEGACYCLE SET (1ST ORDER) | MEGACYCLE (2ND ORDER) | SUPERCYCLE SETS | SUPERCYCLES | CYCLES (3RD ORDER) | RELATIVE CHANGE OF COASTAL ONLAP (LANDWARD 1.0 — 0.5 — BASINWARD 0) | SEQUENCE BOUNDARY AGE | DOWNLAP SURFACE AGE | SYSTEMS TRACTS | EUSTATIC CURVE (250 200 150 100 50 0M) | TIME IN M. YEARS

PHANEROZOIC — UPPER ABSAROKA (UA) — UPPER ABSAROKA A (UAA) — UPPER

UAA-4, UAA-3, UAA-2, UAA-1 (UAB, UAB-1)

LONG TERM; SHORT TERM

B.U. HAQ, P.R. VAIL, J. HARDENBOL, J.F. SARG, B.E. MORGAN

Palaeoclimatol. Palaeoecol. **42**, 65 (1983)]. For the late Jurassic–early Cretaceous (magnetic anomalies M26 through M1), the following profiles were used from the North Pacific: T. W. Hilde, N. Isezaki, J. M. Wageman, *Am. Geophys. Union Geophys. Monogr.* **19**, 205 (1976); and from the western North Atlantic: H. Schouten and K. M. Klitgord, *Earth Planet. Sci. Lett.* **59**, 255 (1982). Magnetic polarity chronozones for the Aptian-Callovian interval are after J. L. LaBrecque *et al.* [*Palaeogeogr. Palaeoclimatol. Palaeoecol.* **42**, 91 (1983)].

19. Pre-Callovian (Triassic through middle Jurassic) synthetic polarity reversal model is based on the following: C. E. Helsley, *Geol. Soc. Am. Bull.* **80**, 2431 (1969); P. J. Burek, *Am. Assoc. Pet. Geol. Bull.* **54**, 1130 (1970); M. W. McElhinny and P. J. Burek, *Nature (London)* **232**, 98 (1971); K. M. Creer, *ibid.* **233**, 545 (1971); D. M. Pechersky and A. N. Khramov, *ibid.* **244**, 499 (1973); C. E. Helsley and M. B. Steiner, *Geol. Soc. Am. Bull.* **85**, 457 (1974); E. Marton, P. Marton, F. Heller, *Earth Planet. Sci. Lett.* **48**, 218 (1980); J. E. T. Channell, J. G. Ogg, W. Lowrie, *Philos. Trans. R. Soc. London Ser. A* **306**, 137 (1982); F. Hörner and F. Heller, *Geophys. J. R. Astron. Soc.* **73**, 705 (1983).

20. Recent studies that have provided direct correlations between the late Cretaceous–Cenozoic fossil occurrences and magnetic polarity reversals include W. B. F. Ryan *et al.*, *Riv. Ital. Paleontol. Stratigr.* **80**, 631 (1974); W. Alvarez *et al.*, *Geol. Soc. Am. Bull.* **88**, 367 (1977); B. U. Haq, W. A. Berggren, J. A. Van Couvering, *Nature (London)* **269**, 483 (1977); H. R. Thierstein *et al.*, *Geology* **5**, 400 (1977); B. U. Haq *et al.*, *ibid.* **8**, 427 (1980); J. E. T. Channell and F. Medizza, *Earth Planet. Sci. Lett.* **55**, 419 (1981); W. Lowrie *et al.*, *Geol. Soc. Am. Bull.* **93**, 414 (1982); R. Z. Poore *et al.*, *Geology* **10**, 508 (1982); H. Stradner and F. Allram, *Init. Rep. Deep Sea Drill. Proj.* **66**, 589 (1982); W. A. Berggren *et al.*, *ibid.* **72**, 675 (1983); G. Napoleone *et al.*, *Geol. Soc. Am. Bull.* **94**, 181 (1983); R. Z. Poore *et al.*, *Palaeogeogr. Palaeoclimatol. Palaeoecol.* **42**, 127 (1983); K. J. Hsü *et al.*, *Geol. Soc. Am. Bull.* **95**, 863 (1984); W. A. Berggren, D. V. Kent, J. J. Flynn, in *The Chronology of the Geological Record*, N. J. Snelling, Ed. (Mem. Geol. Soc. London/Blackwell, Oxford, 1985), vol. 10, p. 141; S. Monechi and H. R. Thierstein, *Mar. Micropaleontol.* **9**, 419 (1985); C. E. Barton and J. Bloemendal, *Init. Rep. Deep Sea Drill. Proj.* **90**, 1294 (1986); W. H. Lohman, *ibid.*, p. 776.

21. H. Bolli, J. B. Saunders, K. Perch-Nielsen, Eds., *Plankton Stratigraphy* (Cambridge Univ. Press, Cambridge, 1985).

22. L. H. Burckle, *Proc. 2nd Work. Group Meet. Int. Geol. Correl. Prog., Proj. 114, Bandung, 1977, Spec. Publ. Geol. Res. Dev. Cen.* **1**, 25 (1978); F. Theyer, C. Y. Mato, S. R. Hammond, *Mar. Micropaleontol.* **3**, 377 (1978); L. H. Burckle and J. Trainer, *Micropaleontology* **25**, 281 (1979); J. A. Barron, in (*21*), pp. 763–809.

23. Direct ties between Jurassic and Cretaceous fossil occurrences and magnetic polarity reversals are provided by the following studies: W. Alvarez *et al.*, *Geol. Soc. Am. Bull.* **88**, 367 (1977); J. E. T. Channell, W. Lowrie, F. Medizza, *Earth Planet. Sci. Lett.* **42**, 153 (1979); W. Lowrie *et al.*, *J. Geophys. Res.* **85**, 3597 (1980); E. Marton, P. Marton, F. Heller, *Earth Planet. Sci. Lett.* **48**, 218 (1980); E. Marton, *ibid.* **57**, 182 (1982); J. E. T. Channell *et al.*, in (*19*); F. Hörner and F. Heller, *J. R. Astron. Soc.* **73**, 705 (1983); J. G. Ogg, *Init. Rep. Deep Sea Drill. Proj.* **76**, 685 (1983); B. Galbrun and L. Rasplus, *C.R. Acad. Sci.* **298**, 219 (1984); T. J. Bralower, *Mar. Micropaleontol.*, in press.

24. H.-J. Anderson *et al.*, *Field Guide Oligocene Excursion, 1969* (Marburg University, Marburg, 1969), p. 47, figure 8; *Giornale Geol.* (Ser. 2), **37**, 69 (1971).

25. To document the Cenozoic sequences, outcrops have been studied in both the northwestern European basins (Anglo-Belgium and Paris basins, southern France, West Germany, and Italy) and along the U.S. Atlantic and Gulf coasts. In Europe the Paleogene sequences have been documented in southern England and the Isle of Wight. This documentation includes the reference section for the Thanetian and the stratotype section of the Bartonian (in Barton area). The Belgian sections include the stratotypes of Ypresian, Ledian, Tongrian, and Rupelian Stages. A northwestern German section near Doberg provided the documentation for the Chattian sequences. In France, the Paris basin area has been of particular significance, and sections studied include the stratotypes or hypostratotypes of the Sparnacian, Cuisian, Lutetian, Auversian, Marinesian, and Stampian

Stages. The sections in southern France include the stratotypes of Aquitanian and Burdigalian (both in the Aquitaine basin). In addition to the Priabonian stratotype (in northern Italy), the extensive literature on Neogene stratotypes and hypostratotypes in Italy and Spain was invaluable in verifying and documenting the chronostratigraphic positions of Neogene sequences. The U.S. sections include Paleogene outcrops along the Atlantic coast in North and South Carolina, and along the Gulf coast in Alabama and Georgia. In addition, Paleogene sequences have also been studied in outcrops on South Island, New Zealand, and along the flanks of the Ottway Mountains in Victoria, Australia.

26. Documentation for the Cretaceous sequences is mainly provided by sections in western and central European basins, the U.S. Gulf coast, and the western interior. In Europe, the lower Cretaceous sequences have been studied in the Suisse Romande area of Switzerland and southeastern France. The Swiss outcrops include the stratotype sections of the Valanginian and Hauterivian Stages. The French localities include lower Cretaceous sections in the Ardeche, Vaucluse, and Alpes de Haute-Provence areas, including the stratotype or hypostratotype sections of the Berriasian, Aptian, Gargasian, Valanginian, Barremian, and Bedoulian. Upper Cretaceous outcrop studies were undertaken in sections in the Alpes Maritimes and the Drome areas of the Provence. In addition, the stratotypes of the Cenomanian (near Le Mans) and Turonian (in the Touraine) and the mid-Cretaceous outcrops of the Boulonnais were also studied. In the United States, the middle and Upper Cretaceous sections have been studied in the western interior and central Texas.

27. The bulk of documentation for the Jurassic sequences came from sections in western Europe, particularly the minor sequences that have been documented only in England and France so far. The English sections include outcrops in Dorset and Somerset in southern England and Yorkshire in northern England. Essentially a complete progression of Jurassic sequences can be seen along the Dorset coast: the Hettangian through Toarcian sequences can be observed from Pinhay Bay eastward to Eastcliff, and the Aalenian through Callovian between Burton Bradstock and Tidmoor Point; the Upper Jurassic and lowest Cretaceous sequences are exposed from the Isle of Portland to Swanage. In France, sequences of Hettangian through early Aalenian age, including the stratotype of Toarcian (near Thouars), have been studied. In addition, sections in southern Germany provided verification of Rhaetian through Toarcian sequences, which include the stratotype section of the Pliensbachian Stage (near Pliensbach). Sections near the Montsalvens area of Switzerland have furnished further confirmation of late Jurassic sequences.

28. Triassic documentation was provided by sections in Svalbard, on the Arctic island of Bjørnøya, in the Dolomites in Italy, and from the Salt Range in Pakistan.

29. J. van Wagoner, in (*10*); P. W. Godwin and E. J. Anderson, *J. Geol.* **93**, 515 (1985).

30. The Jurassic-Cretaceous boundary is placed between the Portlandian and Ryazanian Stages, following the common British usage. Alternative boundary placement (for example, by French stratigraphers) is between the Tithonian and Berriasian Stages. Names of the commonly used suprastage subdivisions included in the stage column (that is, Zechstein, Buntsandstein, Muschelkalk, Lias, Dogger, Malm, Neocomian, and Senonian) are included only for convenience, and no formal status is suggested.

31. The Cenozoic biostratigraphy (Fig. 2) includes planktonic foraminiferal zones as described in the following: W. Blow, *Proc. 1st Int. Conf. Plankton. Microfossils, 1967, Geneva* **1**, 199 (1969); W. A. Berggren in (*12*); R. M. Stainforth, *Univ. Kan. Paleontol. Contrib.* **62**, 1 (1975). Calcareous nannofossil zones are described in E. Martini, *Proc. 2nd Plankton. Conf., 1970, Rome* **2**, 739 (1971); H. Okada and D. Bukry, *Mar. Micropaleontol.* **5**, 321 (1980); D. Bukry, *Soc. Econ. Paleontol. Mineral. Spec. Publ.* **32**, 335 (1981). Radiolarian zones are cited in A. Sanfillipo, M. J. Westberg-Smith, W. R. Riedel, *Init. Rep. Deep Sea Drill. Proj.* **61**, 495 (1981); (*21*), p. 631. Diatom zones are from A. M. Gombos, *Bacillaria* **5**, 225 (1982); _____ and P. Ciesielski, *Init. Rep. Deep Sea Drill. Proj.* **71**, 583 (1983); A. M. Gombos, *ibid.* **73**, 495 (1984); J. Fenner, in (*21*), p. 713; J. A. Barron, *ibid.*, p. 763.

32. F. Robasynski *et al.*, *Rev. Micropaleont.* **26**, 145 (1984).

33. Cretaceous biostratigraphy (Fig. 3) includes: Planktonic foraminiferal zones from I. Premoli-Silva and H. Bolli, *Init. Rep. Deep Sea Drill. Proj.* **15**, 499 (1973); I. Premoli-Silva and A. Boersma, *ibid.* **39**, 615 (1977); J. E. van Hinte, *Am. Assoc. Pet. Geol. Bull.* **60**, 498 (1976); F. Robasynaski *et al.*, *Cah. Micropaleontol.* **1**, 185 (1979); *ibid.* **2**, 181 (1979); M. Caron, in (*21*), p. 17. Calpionellid zones from F. Alleman *et al.*, *Proc. 2nd Plankton. Conf., 1970, Rome*, **2**, 1337 (1971); J. Remane, in *Introduction to Marine Micropaleontology*, B. U. Haq and A. Boersma, Eds. (Elsevier, New York, 1978), p. 161; (*21*), p. 555. Calcareous nannofossil zones from H. Thierstein, *Mar. Micropaleontol.* **1**, 325 (1976); W. Sissingh, *Geol. Mijnbouw* **56**, 37 (1977); H. Manivit *et al.*, *K. Ned. Akad. Wet.* **B80**, 169 (1977); P. H. Roth, *Init. Rep. Deep Sea Drill. Proj.* **44**, 731 (1978); *ibid.* **76**, 587 (1983). Boreal (British) ammonoid-belemnoid zones from P. F. Rawson *et al.*, *Geol. Soc. London Spec. Rep.* **9**, 1 (1978); W. J. Kennedy, *Bull. Geol. Soc. Den.* **33**, 147 (1984). Tethyan ammonoid zones from C. Cavalier and J. Rogers, Eds., *Bur. Rech. Geol. Min. Mem.* **109**, 1 (1980); R. Busnardo, *ibid.* **125**, 293 (1984); F. Amedro, *Rev. Micropaleontol.* **22**, 195 (1980); *Cretaceous Res.* **2**, 261 (1981); *Bull. Soc. Geol. Normandie Amis Mus. Havre* **71**, 17 (1984); B. Clavel *et al.*, *Eclogae Geol. Helv.* **79**, 319 (1986); W. J. Kennedy, cited earlier in this reference; (*32*).

34. Jurassic biostratigraphy section (Fig. 4) includes radiolarian events and preliminary zones in: E. A. Pessagno, *Micropaleontology* **23**, 56 (1977); _____ and C. D. Blome, *ibid.* **26**, 225 (1980); P. O. Baumgartner, *Init. Rep. Deep Sea Drill. Proj.* **76**, 569 (1983); E. A. Pessagno *et al.*, *Cushman Found. Foraminiferal Res. Spec. Publ.*, in press. Calcareous nannofossil zones in T. Barnard and W. W. Hay, *Eclogae Geol. Helv.* **67**, 563 (1974); A. W. Medd, *Mar. Micropaleontol.* **7**, 73 (1982); G. B. Hamilton, in *A Stratigraphical Index of Calcareous Nannofossils*, A. R. Lord, Ed. (Horwood, Chichester, England, 1982), p. 17; P. H. Roth, A. W. Medd, D. K. Watkins, *Init. Rep. Deep Sea Drill. Proj.* **76**, 573 (1983). Boreal (British) ammonoid zones in J. C. W. Cope *et al.*, *Geol. Soc. London Spec. Rep.* **14**, 73 (1980); *ibid.* **15**, 109 (1980).

35. Triassic biostratigraphy (Fig. 5) includes radiolarian zones in C. D. Blome, *Bull. Am. Paleontol.* **85**, 5 (1984). Conodont zones in L. C. Mosher, *J. Paleontol.* **44**, 737 (1970); W. C. Sweet *et al.*, *Geol. Soc. Am. Mem.* **127**, 441 (1971); T. Matsuda, in *The Tethys, Her Paleogeography and Paleobiogeography from Paleozoic to Mesozoic*, K. Nakazawa and J. M. Dickens, Eds. (Tokai Univ. Press, Tokyo, 1985), p. 157. The Tethyan ammonoid zones in E. T. Tozer, *Geol. Surv. Can. Misc. Rep.* **35**, 8 (1984). North American ammonoid zones after N. J. Silbering and E. T. Tozer, *Geol. Soc. Am. Spec. Pap.* **110**, 7 (1968).

36. The cycle charts include palynomorph (mostly dinoflagellate) biohorizons that have been synthesized and compiled by EPR palynologists (L. E. Stover, M. Millioud, N. S. Ioannides, R. Jan du Chêne, Y. Y. Chen, J. D. Shane, and B. E. Morgan).

37. The cycle terminology adopted here (that is, Absaroka, Zuni, Tejas, and their subdivisions) is based on the sequence terminology suggested by L. L. Sloss, in (*3*).

38. The dashed lines drawn through the condensed sections represent the surfaces of maximum flooding (downlap surfaces on seismic profiles). However, the relative thickness of these lines represents the relative magnitude of the condensed sections associated with these surfaces.

39. The magnitude of long-term sea level variations on the curves is estimated, as in the method described by J. Hardenbol, P. R. Vail, and J. Ferrer [*Oceanol. Acta* **4** (suppl.), 31 (1981)], with a high value (in Campanian) adopted from the estimate of C. G. A. Harrison [in *Sea Level Change*, R. Revelle, Ed. (National Research Council, Washington, DC, in press)]. The magnitude of short-term sea level rises and falls has been estimated from seismic and sequence-stratigraphic data.

40. T. A. Davies, W. W. Hay, J. R. Southam, T. R. Worsley, *Science* **197**, 53 (1977); T. R. Worsley and T. A. Davies, *ibid.* **203**, 455 (1979).

41. J. A. Barron and G. Keller, *Geology* **10**, 577 (1982); G. Keller and J. A. Barron, *Geol. Soc. Am. Bull.* **94**, 590 (1983); *Geology*, in press.

42. L. A. Mayer, T. H. Shipley, E. L. Winterer, *Science* **233**, 761 (1986).

43. W. H. Berger and E. L. Winterer, *Spec. Publ. Int. Assoc. Sedimentol.* **1**, 11 (1974).

44. B. U. Haq, *Mar. Geol.* **15**, M25 (1973).

45. The Mesozoic and Cenozoic cycle charts presented in Figs. 2 through 5 are the product of input and interest of many colleagues, both inside and outside EPR. The principal responsibility for the chronoeustatic framework, however, rested with the authors of this article. Input for the individual cycle charts varied; the collaborators are listed at the bottom of each cycle chart. We are grateful to all of these participants and to many other colleagues for their important input, without which this synthesis would have been far less detailed. We thank R. G. Todd and J. M. Widmier for their support for an accurate global stratigraphic-eustatic framework and for stimulating discussions on the subject. The charts were drafted by D. Thornton. We thank Exxon Production Research Company for giving us permission to release the cycle charts and to publish this article.

Fertility Policy in China: Future Options

SUSAN GREENHALGH AND JOHN BONGAARTS

A wide range of social, economic, and demographic criteria are used to evaluate China's present one-child policy and five alternative fertility policies that might guide China's population control efforts until the end of the century when the one-child policy is scheduled to be abandoned. These criteria include the policies' macrodemographic impact on total population size and population aging; their microdemographic effects on the family's ability to support the elderly, its economic capabilities, and the position of women; and their cultural acceptability to the majority Han Chinese population. The results suggest that the least desirable strategy is to retain the present policy; all the two-child alternatives perform better than the current one-child policy in achieving the policy goals considered.

SINCE CHINA FIRST ADOPTED STRONG BIRTH CONTROL POLIcies in the early 1970s, there has been a dramatic fall in Chinese fertility. Under the *wan xi shao* policy (literally "late, sparse, and few," a policy calling for later childbearing, longer spacing, and fewer children) in effect during the 1970s, the total fertility rate, the most widely used fertility measure, dropped from 5.93 births per woman in 1970 to 2.66 births in 1979 (*1*). The one-child policy introduced in 1979 has pushed fertility even lower: by 1984 the total fertility rate had dropped to 1.94, slightly below the level required for population replacement (*2*).

In part because of the policies' demographic success and in part because of the political problems that stemmed from efforts to shrink family size very rapidly, in 1984 and 1985 China's leaders took steps to relax birth-planning policy. An important shift in policy direction occurred in April 1984 with the issuance of Central Document 7 by the Party's Central Committee. (Central Committee documents on various issues are numbered from 1 each year.) Under this document the conditions under which couples may have two children were expanded and reforms were called for in policy, work style, organization, and ideology that were designed to increase voluntary participation through better meshing of the policy with the needs of the people (*3*). Further relaxation occurred in early 1985, when the Central Committee changed its target for the year 2000 from 1.2 billion to about 1.2 billion—an apparently small change, but one that indicates a notable increase in flexibility on the critical issue of population goals.

In May 1986 concern that changes in the age structure would put upward pressure on the birthrate during the coming decade was reflected in Document 13, which supersedes Document 7 as the guiding statement on fertility policy (*4*). Although many of the moderate elements introduced by Document 7 are continued in this directive, its central message appears to be that cadres must take stronger measures to ensure that birth targets are met during the seventh 5-year plan period (1986 to 1990). In late 1986 mounting evidence that fertility was rising after several years of decline led Premier Zhao Ziyang to advocate in an early December speech that a renewed emphasis be placed on the one-child limitation (*5*). Despite these indications that the policy is becoming more restrictive again, the question of which elements from the more relaxed phase can be maintained in the late 1980s and the 1990s without jeopardizing achievement of the century-end target appears unresolved at the political center. The optimal mix of policy elements is also the subject of a lively debate among scholars.

From speeches and articles that have been published in the past few years, it is clear that the range of factors considered in population policy-making continues to widen. The sparse evidence available from the 1970s suggests that one macrodemographic consideration—total population size—dominated the decision to initiate the one-child policy in 1979. Although population quantity, combined with population quality, remain the central considerations in the mid-1980s, several new concerns have also been raised in academic and official circles: the cultural acceptability of fertility policy, its effects on the physical safety of females, and its impact on the rate of population aging (*6*).

Were these new considerations to be brought directly to bear on fertility policy, it is not clear what shape that policy would take. Not wishing to abandon the one-child policy for both substantive and political reasons, China's leaders have tended to incorporate new factors only by tinkering with the preexisting policy. With the benefits of hindsight and the perspective of outsiders, we use these new criteria and other factors to evaluate the present policy and five alternative policies that might guide China's population control efforts until the end of the century, when the one-child policy is scheduled to be abandoned. We consider the macrodemographic impact of these hypothetical policies on total population size and population aging; the microdemographic effects on the family's ability to support the elderly, its economic capabilities, and the socioeconomic position of women (two factors Chinese leaders do

The authors are associate and senior associate, respectively, of the Center for Policy Studies, The Population Council, 1 Dag Hammarskjold Plaza, New York, NY 10017.